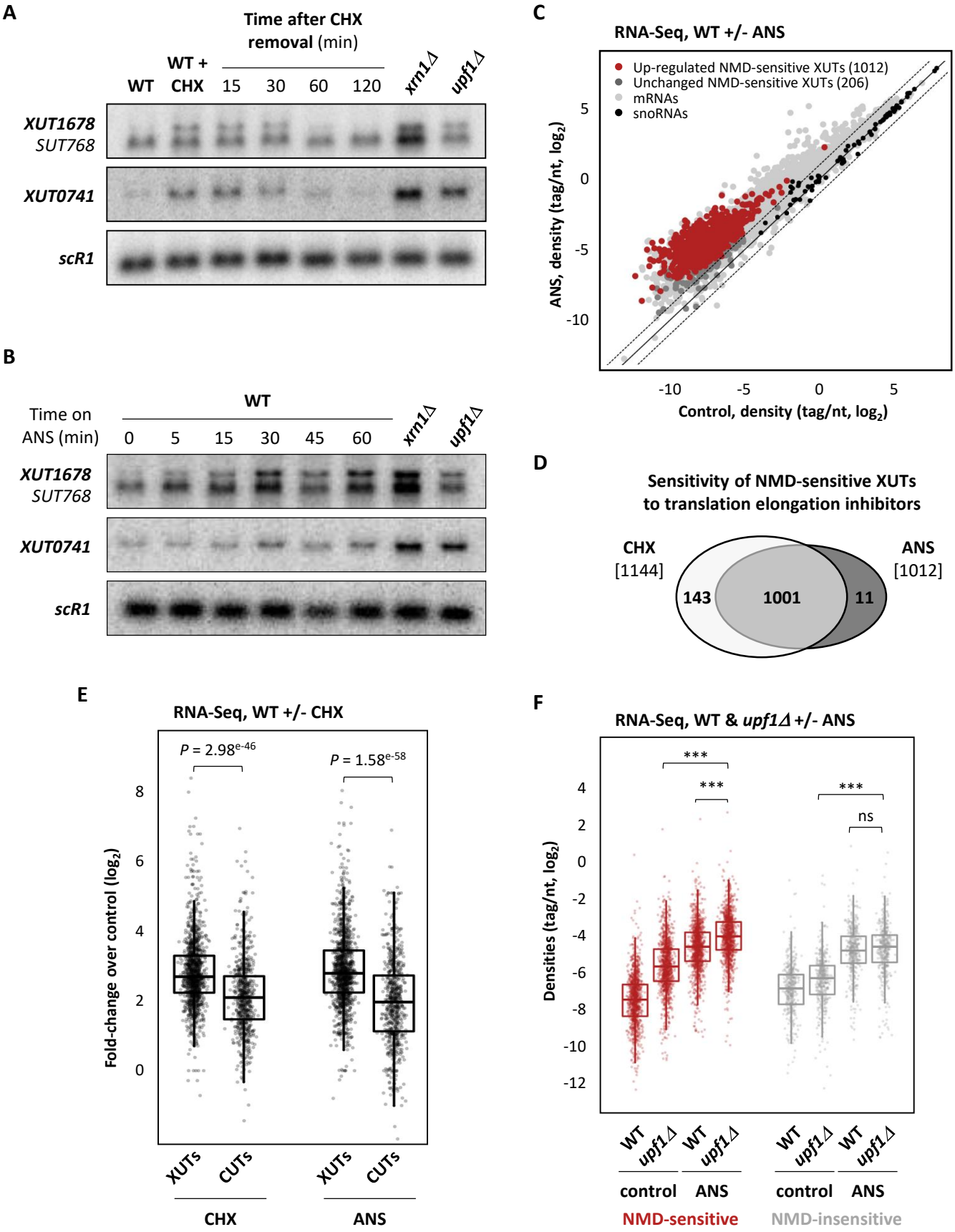

Figure S1. NMD-sensitive lncRNAs accumulate upon translation inhibition.

A. WT (YAM1), *xrn1Δ* (YAM6) and *upf1Δ* (YAM202) cells were grown to mid-log phase in rich (YPD) medium at 30°C. CHX was then added to the WT cells for 15 min (100 µg/ml, final concentration). The CHX-treated cells were then washed with fresh pre-heated YPD medium and re-incubated at 30°C. Samples of washed cells were collected after 15, 30, 60 and 120 min. Total RNA was extracted and analysed by Northern blot. *XUT1678* (and the overlapping *SUT768*), *XUT0741* and *scR1* (loading control) were detected using ^{32}P-labelled AMO1595, AMO1762 and AMO1482 oligonucleotides, respectively.

B. WT (YAM1) cells were grown to mid-log phase in rich (YPD) medium at 30°C. ANS was then added at a final concentration of 100 µg/ml, and samples were collected at different time points. Untreated *xrn1Δ* (YAM6) and *upf1Δ* (YAM202) cells, grown under the same conditions, were used as controls. Total RNA was extracted and analysed by Northern blot as above.

(legend continued on next page)

Figure S1. NMD-sensitive lncRNAs accumulate upon translation inhibition *(continued).*

C. Total RNA-Seq was performed using total RNA extracted from exponentially growing WT (YAM1) cells (grown as above) treated for 30 minutes with ANS (100 µg/ml, final concentration) or with an equal volume of DMSO (control). The scatter plot shows the RNA-Seq signals (tag densities, $\log_2$ scale) for the NMD-sensitive XUTs, mRNAs (light grey dots) and snoRNAs (black dots) in ANS-treated and control WT cells. Up-regulated (ANS/control fold-change >2, *P*-value <0.05) and unaffected NMD-sensitive XUTs are represented as red and dark grey dots, respectively (see also Table S1).

D. Venn diagram showing the number of NMD-sensitive XUTs that accumulate in CHX- and/or ANS-treated WT cells (see also Table S1).

E. Sensitivity of NMD-sensitive XUTs and CUTs to CHX and ANS. The box-plot shows the global sensitivity to CHX (left) and ANS (right) of NMD-sensitive XUTs and 'strict' CUTs, in WT cells (drug/control ratio of RNA-Seq signals). The 'strict' CUTs correspond to a subgroup of CUTs (661) that do not overlap an annotated XUT.

F. Total RNA-Seq was performed in WT (YAM1) and *upf1Δ* (YAM202) cells treated for 30 minutes with ANS (100 µg/ml, final concentration) or an equal volume of DMSO. The box-plot shows the densities (tag/not, $\log_2$) computed for the NMD-sensitive and NMD-insensitive XUTs. *** *P*-value < 0.001; ns, not significant upon two-sided Wilcoxon rank-sum test (adjusted for multiple testing with the Benjamini–Hochberg procedure).

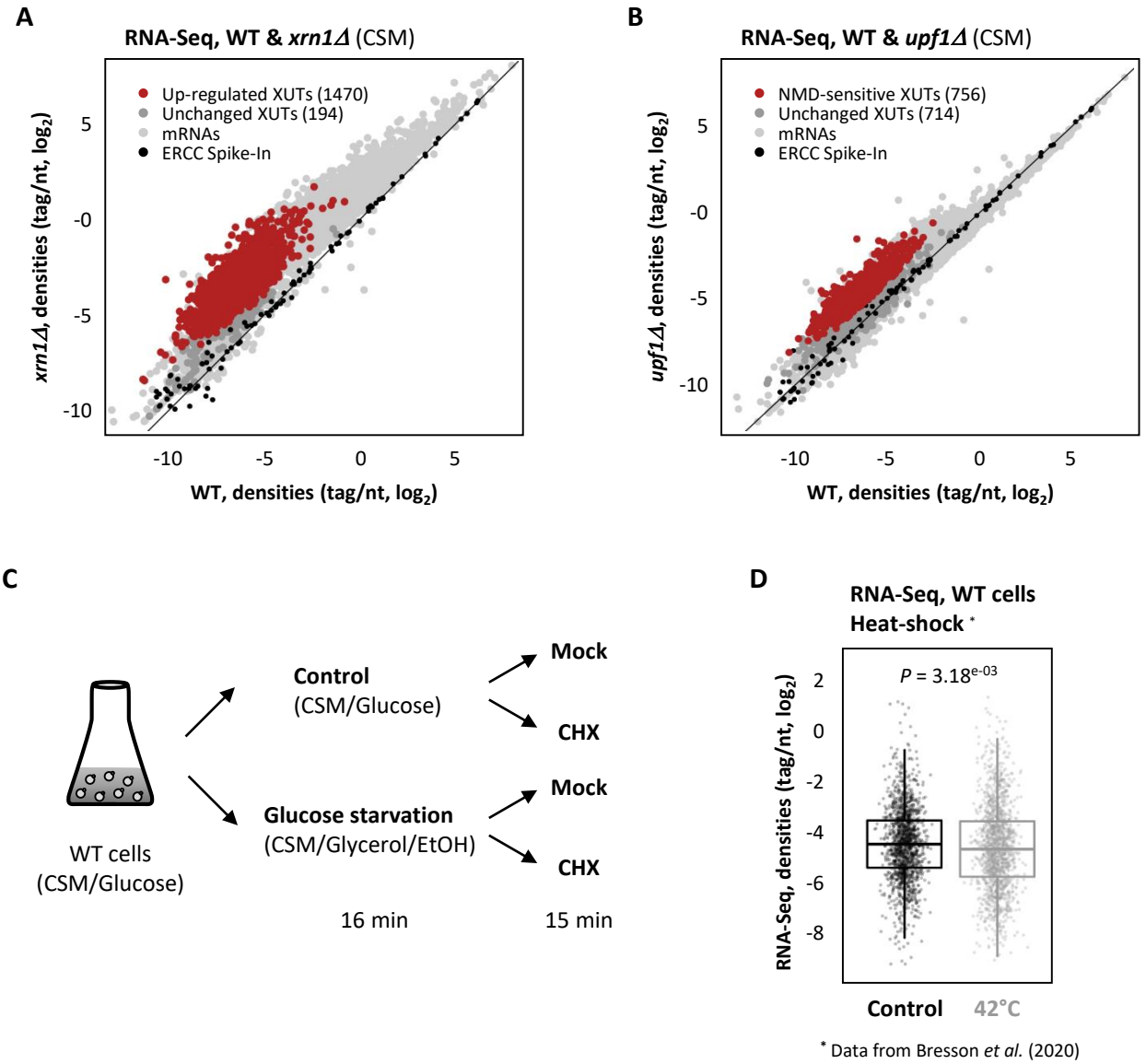

Figure S2. XUTs levels remain unaffected upon translation initiation inhibition.

A. XUTs landscape in CSM medium. Total RNA-Seq was performed in WT (YAM1) and *xrn1Δ* (YAM6) cells grown to mid-log phase in Complete Synthetic Medium (CSM). Densities (tag/not, log_2) were computed for XUTs, mRNAs (light grey dots) and snoRNAs (black dots). The 1470 XUTs up-regulated in the *xrn1* mutant (*xrn1Δ*/WT fold-change >2, *P*-value <0.05) are highlighted in red. The dark grey dots correspond to the other XUTs, the expression of which is not significantly affected.

B. Landscape of NMD-sensitive XUTs in CSM medium. Same as above, using WT (YAM1) and *upf1Δ* (YAM202) cells grown in CSM. The red dots represent the 756 XUTs defined as NMD-sensitive in this condition (*upf1Δ*/WT fold-change >2, *P*-value <0.05).

C. Experimental scheme. WT (YAM1) cells were grown to mid-log phase in CSM with glucose as carbon source, and then shifted for 16 min in CSM where glucose was replaced by glycerol and ethanol (glucose starvation). In parallel, control cells were maintained for the same time in glucose-containing CSM. CHX (100 µg/ml final concentration) or an equal volume of DMSO (Mock) was then added to each sample. Cells were harvested after 15 min of treatment; then total RNA was extracted. Note that the CSM medium used here is different from the rich medium (YPD) that was originally used to annotate XUTs, so that we had to re-define the XUTs landscape in CSM (see above).

D. Analysis of published RNA-Seq data obtained in WT cells grown in CSM and then shifted for 16 min at 42°C (Bresson *et al.*, 2020). Densities (tag/nt, log_2) were computed for the 1470 XUTs expressed in CSM (see panel A). The indicated *P*-value was obtained upon two-sided Wilcoxon rank-sum test.

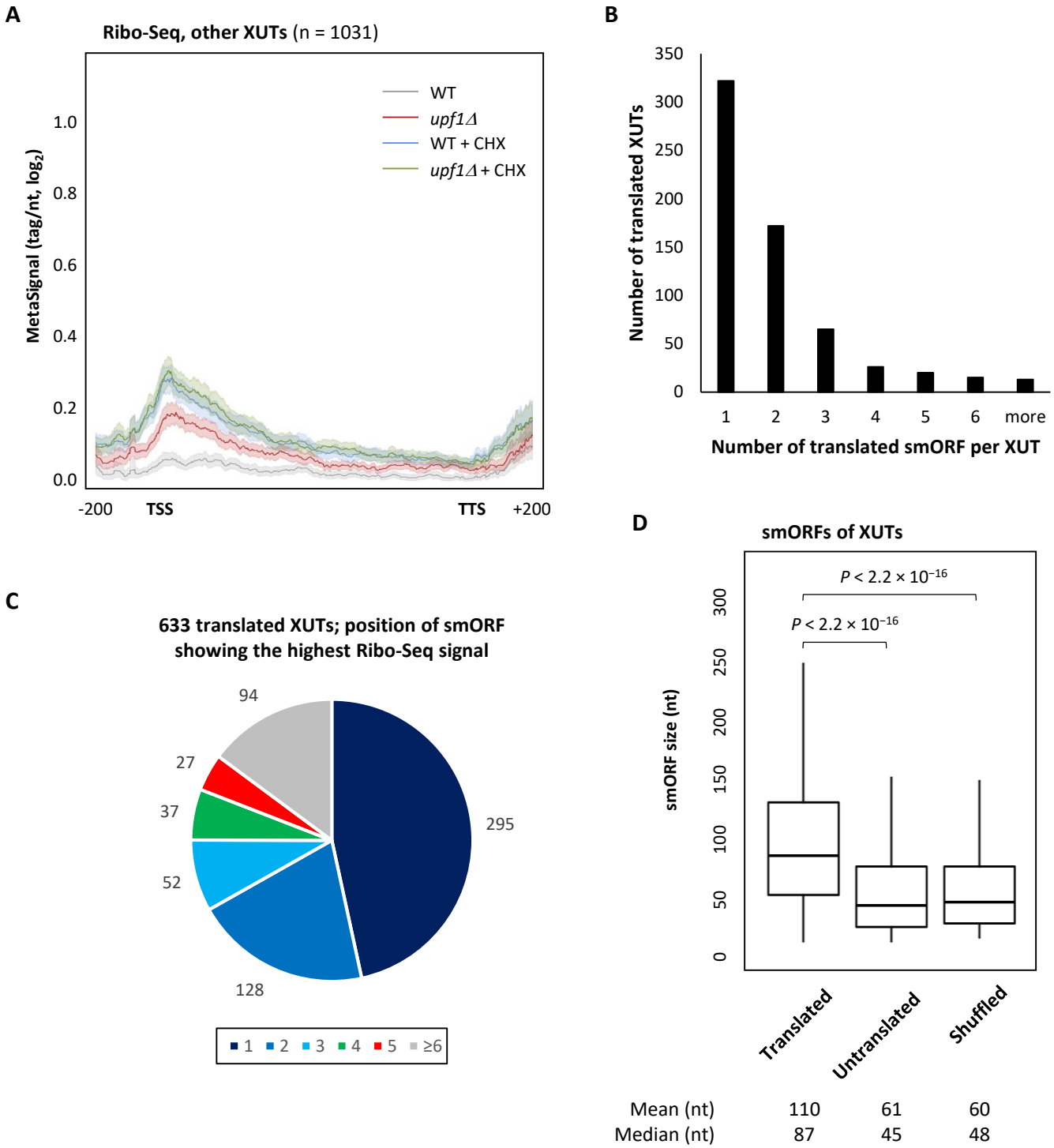

Figure S3. Translational landscape of XUTs.

A. Metagene of Ribo-Seq signals along the 1031 XUTs that were not detected as translated upon analysis using the Ribotricer method, separating the different conditions (*i.e.* XUTs excluded from list 2). For each condition, the densities (tag/nt, $\log_2$) along the XUTs +/- 200 nt were piled up, then the average signal was plotted. The shading surrounding each line denotes the 95% confidence interval.

B. Histogram showing the number of translated smORFs per XUTs (for the 1270 smORFs and 633 XUTs of list 2).

C. Pie chart showing for the 633 translated XUTs (list 2) the position of the smORF with the highest Ribo-Seq signal relative to all the smORFs predicted across the XUT sequence (≥ 5 codons, starting with an AUG).

D. Box-plot showing the size of the 1270 translated smORFs of XUTs (list 2) compared to the other untranslated ORFs (≥ 5 codons, starting with an AUG) found in XUTs and to the three first ORFs found by chance when randomly shuffling the sequence of XUTs (100 random shuffling per XUT, preserving the nucleotide content). The mean and median values for each category are indicated. The *P*-values were obtained upon two-sided Wilcoxon rank-sum test (adjusted for multiple testing with the Benjamini–Hochberg procedure).

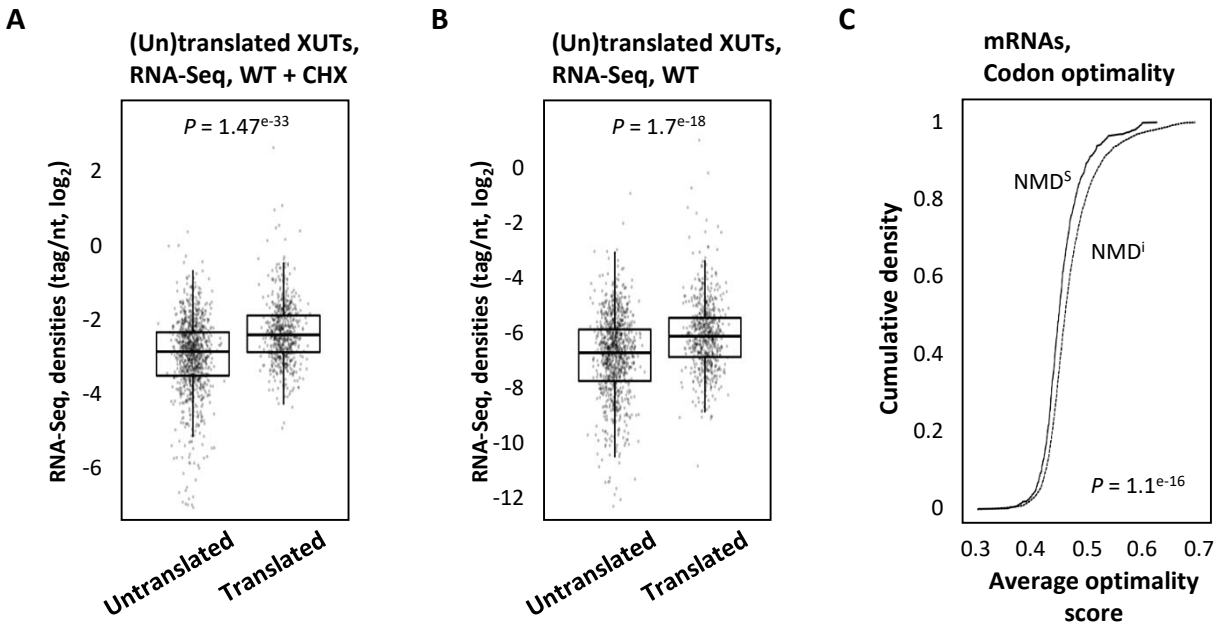

Figure S4. Features of translated XUTs

A. RNA-Seq signals in CHX-treated WT cells for the XUTs detected as translated (633) or not (1031). The *P*-value was obtained upon two-sided Wilcoxon rank-sum test.

B. Same as above in untreated WT cells.

C. Average codon optimality score for the NMD-sensitive (NMD^S, full line, n = 833) and NMD-insensitive (NMD^i, dashed line, n = 4667) mRNAs, shown as a cumulative frequency plot. The indicated *P*-value was obtained upon Kolmogorov–Smirnov test.

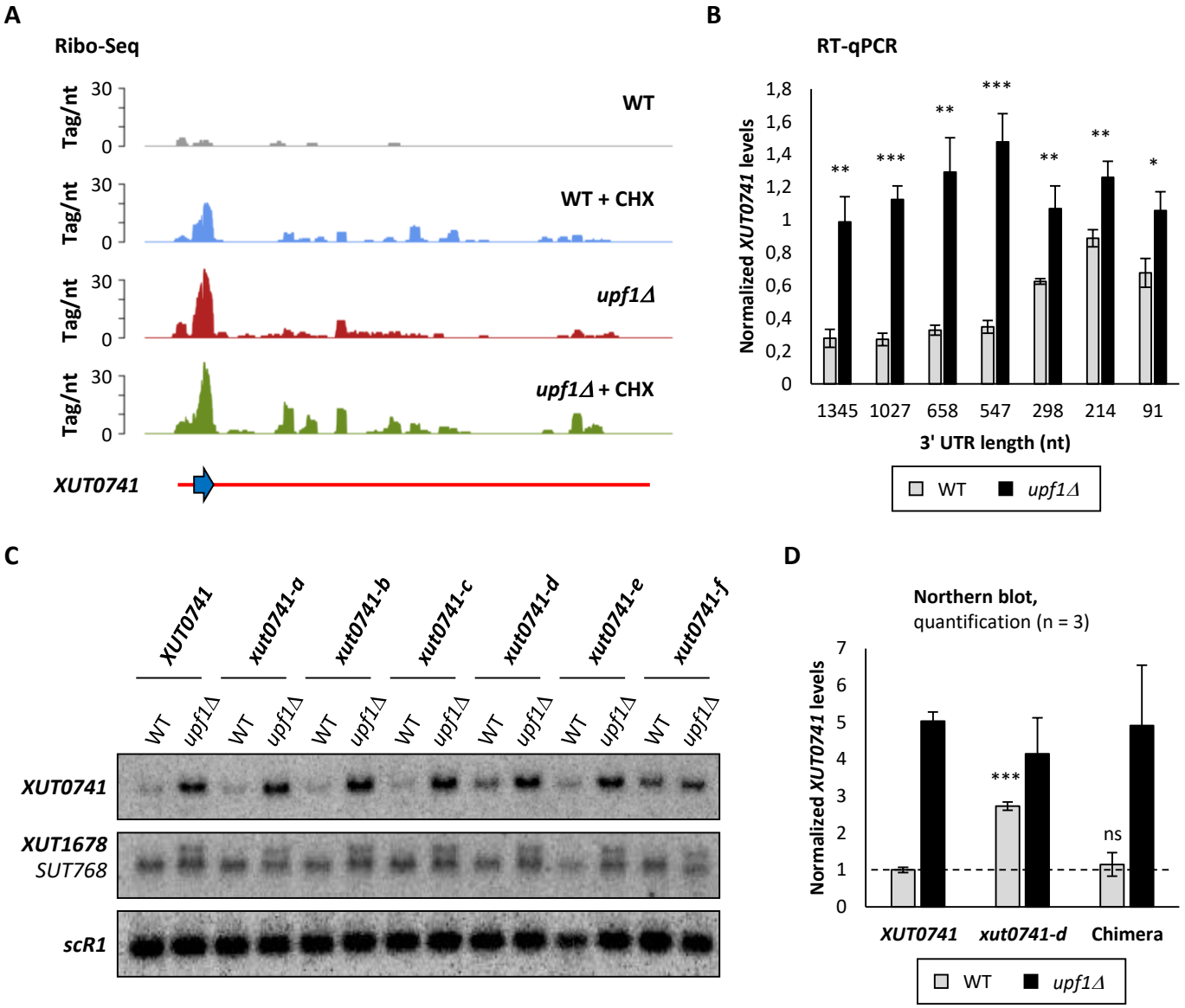

Figure S5. The NMD-sensitivity of *XUT0741* depends on its long 3' UTR.

A. Snapshot of Ribo-Seq signals across *XUT0741* in WT and *upf1Δ* cells, with or without CHX treatment. For each condition, the signals (tag/nt) obtained for the two biological replicates were added. *XUT0741* is depicted as a red line. The blue arrow represents the single smORF detected as actively translated in our analysis.

B. WT and *upf1Δ* cells expressing the different alleles of *XUT0741* (see Figure 6A) were grown to mid-log phase at 30°C in YPD medium. After total RNA extraction, the levels of each transcript were assessed by strand-specific RT-qPCR, and then normalized on *scR1*. The black and grey bars represent the mean values +/- SD in WT (grey) and *upf1Δ* (black) cells, calculated from three independent biological replicates. $^{*}P < 0.05$; $^{**}P < 0.01$; $^{***}P < 0.001$ upon t-test.

C. The same RNAs as above were analyzed by Northern blot. *XUT0741*, *XUT1678* (and the overlapping *SUT768*) and *scR1* (loading control) were detected using ^{32}P-labelled AMO1762, AMO1595 and AMO1482 oligonucleotides, respectively.

D. WT and *upf1Δ* cells expressing the native *XUT0741*, the *xut0741-d* allele and the chimera were grown as described above. Total RNA was extracted and analyzed by Northern blot. The different alleles of *XUT0741* and *scR1* (loading control) were detected by Northern blot using ^{32}P-labelled AMO3581 and AMO1482 oligonucleotides, respectively. Mean and SD values were calculated from three independent biological replicates. The average level of the native *XUT0741* in WT cells was set to 1. $^{***}P < 0.001$; ns, not significant upon t-test.

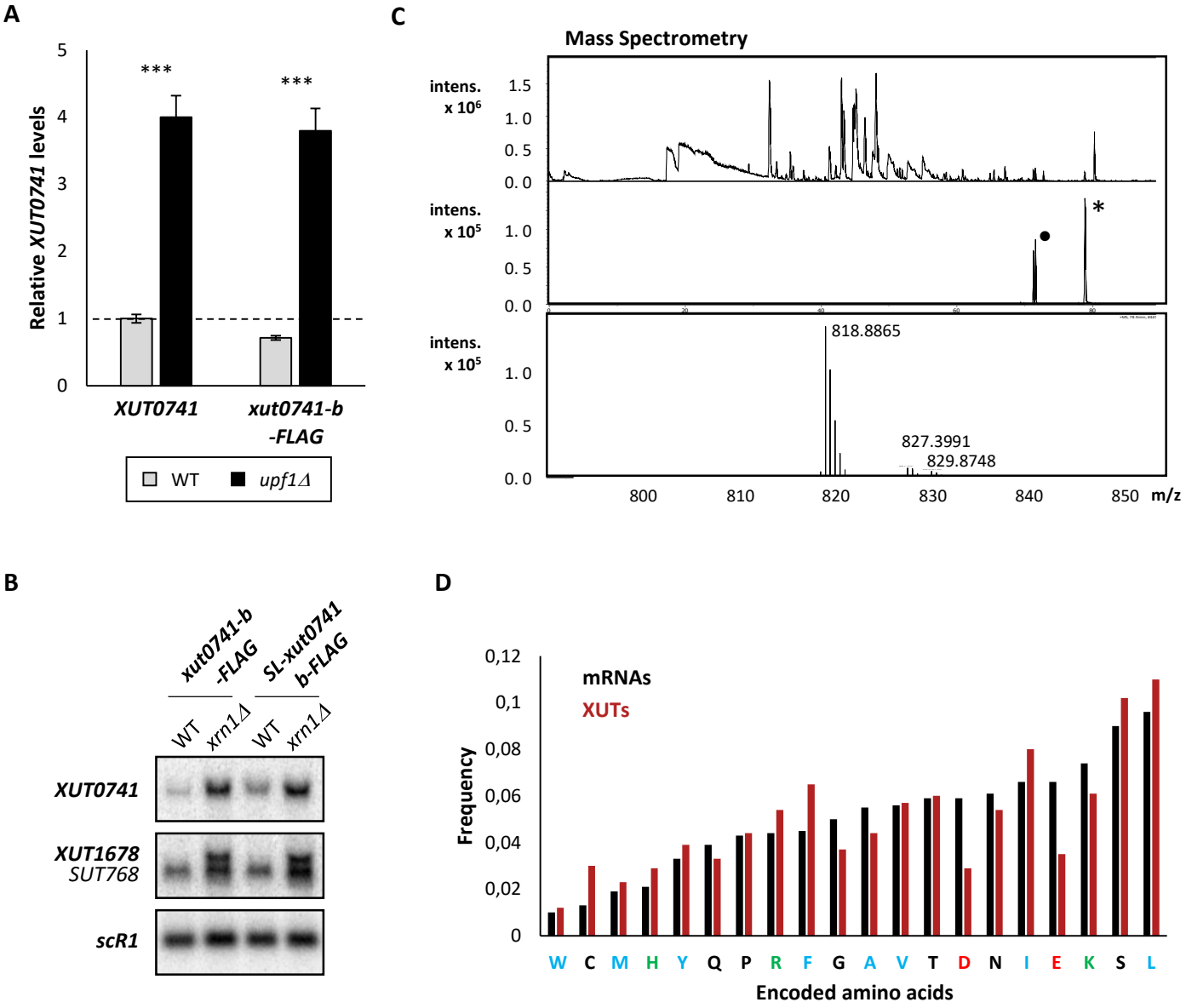

Figure S6. Detection of the peptide derived from an NMD-sensitive XUT reporter.

A. WT and *upf1Δ* cells expressing the native *XUT0741* or the *xut0741-b* allele fused to a C-terminal 3FLAG tag (*xut0741-b-FLAG*) were grown to mid-log phase, at 30°C, in YPD medium. Total RNA was extracted and analyzed by strand-specific RT-qPCR. Levels of *XUT0741* transcripts were normalized on *scR1*. Mean and SD values were calculated from three independent biological replicates. *** $P < 0.001$ upon t-test. Dashed line: WT levels of *XUT0741* set as 1.

B. WT and *xrn1Δ* cells expressing the *xut0741-b-FLAG* or the *SL-xut0741-b-FLAG* alleles were grown as above. Total RNA was extracted and analysed by Northern-blot. *XUT0741*, *XUT1678* (and the overlapping *SUT768*) and *scR1* (loading control) were detected as described above.

C. Mass spectrometry analysis of the 1-10 kDa gel fraction from *upf1Δ* (YAM202) cells grown in the presence of MG132 proteasome inhibitor, spiked with the *XUT0741* heavy synthetic peptide. Base peak chromatogram (upper panel) and MS extracted-ions chromatogram (XIC) of the *XUT0741* labelled peptide (m/z = 818.88) marked with an asterisk (middle panel) are showed. Mass spectrum (lower panel) acquired at the retention time of the heavy synthetic peptide show the absence of peak at lower mass (m/z = 815.4) corresponding to its endogenous counterpart. Chromatographic peak marked with bold circle corresponds to ion interference.

D. Frequency of amino acids encoded by the ORFs of mRNAs (black bars) or the smORFs of XUTs (red bars). The smORF with the highest Ribo-Seq signal was considered for XUTs with several annotated smORFs. Hydrophobic, positively charged and negatively charged residues are indicated in blue, green and red respectively. The other residues are in black.

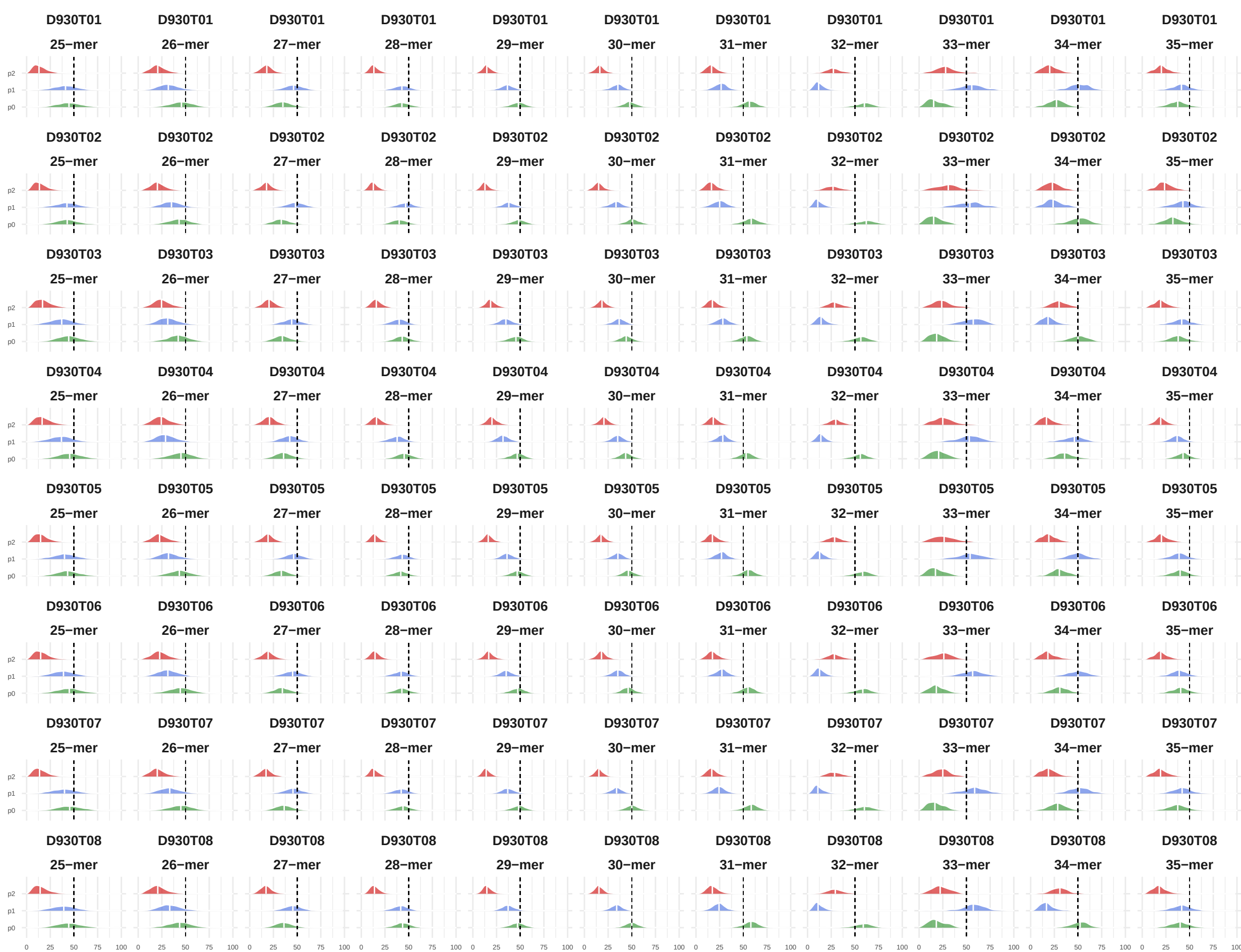
D930T01 25–mer
D930T01 26–mer
D930T01 27–mer
D930T01 28–mer
D930T01 29–mer
D930T01 30–mer
D930T01 31–mer
D930T01 32–mer
D930T01 33–mer
D930T01 34–mer
D930T01 35–mer
D930T02 25–mer
D930T02 26–mer
D930T02 27–mer
D930T02 28–mer
D930T02 29–mer
D930T02 30–mer
D930T02 31–mer
D930T02 32–mer
D930T02 33–mer
D930T02 34–mer
D930T02 35–mer
D930T03 25–mer
D930T03 26–mer
D930T03 27–mer
D930T03 28–mer
D930T03 29–mer
D930T03 30–mer
D930T03 31–mer
D930T03 32–mer
D930T03 33–mer
D930T03 34–mer
D930T03 35–mer
D930T04 25–mer
D930T04 26–mer
D930T04 27–mer
D930T04 28–mer
D930T04 29–mer
D930T04 30–mer
D930T04 31–mer
D930T04 32–mer
D930T04 33–mer
D930T04 34–mer
D930T04 35–mer
D930T05 25–mer
D930T05 26–mer
D930T05 27–mer
D930T05 28–mer
D930T05 29–mer
D930T05 30–mer
D930T05 31–mer
D930T05 32–mer
D930T05 33–mer
D930T05 34–mer
D930T05 35–mer
D930T06 25–mer
D930T06 26–mer
D930T06 27–mer
D930T06 28–mer
D930T06 29–mer
D930T06 30–mer
D930T06 31–mer
D930T06 32–mer
D930T06 33–mer
D930T06 34–mer
D930T06 35–mer
D930T07 25–mer
D930T07 26–mer
D930T07 27–mer
D930T07 28–mer
D930T07 29–mer
D930T07 30–mer
D930T07 31–mer
D930T07 32–mer
D930T07 33–mer
D930T07 34–mer
D930T07 35–mer
D930T08 25–mer
D930T08 26–mer
D930T08 27–mer
D930T08 28–mer
D930T08 29–mer
D930T08 30–mer
D930T08 31–mer
D930T08 32–mer
D930T08 33–mer
D930T08 34–mer
D930T08 35–mer
p2
p1
p0
0 25 50 75 100

Figure S7. Phasing of Ribo-Seq data.
For each dataset, the P-site of the different k-mers (25-mers to 35-mers) was predicted with RiboWaltz (Lauria *et al.*, 2018). As a quality control, for each k-mer, we calculated for the protein-coding genes the fraction of reads that are in-frame with the expected ORF (mentioned as P0). D930T01-02 : WT – native conditions, replicates 1-2 ; D930T03-04 : WT – CHX, replicates 1-2 ; D930T05-06 : *upf1Δ* – native conditions, replicates 1-2 ; D930T07-08 : *upf1Δ* – CHX, replicates 1-2.